Acta of Bioengineering and Biomechanics
Vol. 26, No. 3, 2024

Original paper
DOI: 10.37190/ABB-02436-2024-02

Biomechanical study of elbow joint: different stages after the elbow anterior capsule injury

FANG WANG[1]*, BOTIAN TIAN[1], MINGXIN LI[2], XINJIE CHANG[1], YUBO FAN[3,4]

[1] College of Mechanical Engineering, Tianjin University of Science and Technology, Tianjin, China.
[2] Department of Traumatic Orthopaedics, Tianjin Hospital, Tianjin, China.
[3] Key Laboratory for Biomechanics and Mechanobiology of Ministry of Education.
[4] School of Biological Sciences and Medical Engineering, Beihang University, Beijing, China.

Purpose: Elbow contracture is a common complication post-elbow trauma, the biomechanical environment after anterior capsule injury was complex. This study aimed to use a finite element model to investigate the biomechanical environment within elbow capsule and its surrounding tissues at various stages after anterior capsule injury. *Methods*: A finite element model of the elbow joint, incorporating muscle activation behavior, was developed to simulate elbow flexion under normal condition (no injury) and at 2, 4, 6 and 8 weeks following anterior joint capsular injury. The model was used to analyze von Mises stress distribution and changes within the elbow tissues. *Results*: At no injury condition, and 2, 4, 6 and 8 weeks, the stress of the anterior articular capsule at 60° flexion were 2.62, 3.87, 4.40, 4.57 and 5.24 MPa, respectively. Under normal conditions, and at 2, and 4 weeks, the ulnar cartilage attained its peak stress at 75°. In normal conditions, the highest stress in the ulnar cartilage was 1.08 MPa, amounting to 1.02 times and 1.05 times the stress observed at 2 and 4 weeks, respectively. At 4 weeks, compared with 6 weeks, the stress of the anterior bundle at 15, 30, 45 and 60° was reduced by 11.1, 22.6, 37.3 and 36.1%, respectively. At 6 and 8 weeks, the peak stress in the posterior articular capsule reached 11.5 and 11.7 MPa, respectively, showing minimal variation. *Conclusions*: The results could offer theoretical basis for rehabilitation professionals in treating and preventing elbow capsule contracture.

Key words: *anterior articular capsule, computational elbow model, flexion, capsular contracture, simulation approach*

1. Introduction

Elbow contracture is a common complication post-elbow trauma [21], occurred at a rate of 50% [12]. Research indicated that joint contracture can reduce elbow motion range by 50% and upper limb functionality by 80% [27], impacting gait stability. The emergence and progression of elbow contracture not only limit a patient's ability to perform activities but can also result in the loss of work capacity, being a serious burden on the patient.

Capsular contracture increased the stiffness of the articular capsule and restricted passive range of motion (ROM) of the joint [30]. Posttraumatic contracture is typified by capsular thickening and fibrosis [33], hindering the elbow's ability to execute daily tasks. During capsular contractures, due to alpha-smooth muscle actin (α-SMA) higher level expression, fibroblasts in the articular capsule were transformed into myofibroblasts [38], experiment suggested a significant role of myofibroblasts in post-traumatic elbow exogenous contracture [17]. The pathogenesis of joint contracture remains ambiguous [36], mechanical factors are known to influence it [32]. Hinz et al. [18] noted that myofibroblast activation post tissue injury and alterations in the mechanical microenvironment were primary drivers of myofibroblast genesis.

Currently, stretching is the predominant non-surgical approach for both preventing and treating joint con-

* Corresponding author: Fang Wang, College of Mechanical Engineering, Tianjin University of Science and Technology, Tianjin, China. E-mail: fwang@tust.edu.cn
Received: April 15th, 2024
Accepted for publication: September 8th, 2024

tracture. Due to complex biomechanical environment after anterior capsule injury, the outcome of stretching treatment made an obvious difference. Veltman et al. [35] used dynamic splint to treat 72 patients with elbow extension and flexion contracture and observed significant improvement in elbow extension and flexion. However, Adolfsson [1] found that stretching was not effective in treating elbow capsular contracture at the late phase. During joint capsular contracture, the biomechanical environment of elbow internal tissues is dynamic, understanding that can hold significant value in treating capsular contracture and devising rehabilitation programs [2]. Finte element can provide a deeper knowledge about complex biomechanical environment. For example, Kahmann et al. [20] explored elbow biomechanical environment under loads for daily living by finite model.

This paper established a finite element model of the elbow joint encompassing muscle activation behavior, bone and soft tissue. By simulating flexion motion at 2, 4, 6, and 8 weeks post normal condition (no injury) and anterior capsular injury, we analyzed the von Mises stress distribution and changes in elbow joint tissues at these intervals. Additionally, we evaluated the mechanical environment within the elbow capsule and surrounding tissues at different contracture stages. This could assist rehabilitation physicians in preventing and treating joint contracture and in providing a reference.

2. Materials and methods

2.1. Establishment of the elbow joint finite element model

A 43-year-old male volunteer, measuring 176 cm in height and weighing 77 kg, with no upper limb malformations or history of elbow trauma, was recruited. The volunteer consented to participate in the study and signed an informed consent form. For the CT scan, the left upper limb was positioned at a 90° neutral angle. The scan commenced at the distal humerus and concluded at the proximal ulna and radius. The CT images had a thickness of 1 mm and a resolution of 256 × 256 pixels, yielding a total of 229 image sequences.

The CT imaging data were imported into Mimics 21.0 (Materialise Inc., Leuven, Belgium). Owing to the varying grayscale values of elbow soft tissues in CT scans, only the humerus, radius, and ulna 3D models were extracted using the software. These initial models were then refined using Geomagic 2017 (3D Systems Inc., NC, USA). Subsequently, hexahedral solid element meshing of the smoothed elbow joint skeleton model was conducted in Hypermesh 2019 (Altair Engineering, Inc., USA). With orthopedic guidance, soft tissues such as the articular cartilage, articular capsule, medial collateral ligament (MCL), annular ligament (AL), radial collateral ligament (RCL), lateral ulnar collateral ligament (LUCL), and associated muscles were modeled. Soft tissue components unattached to bone were constructed with hexahedral solid units, while those attached to bone were connected using pentahedral solid units with common nodes. The resulting finite element model, depicted in Fig. 1, consisted of 32113 nodes and 27061 elements: 23460 elements for bones, 24447 elements for the articular capsule, 904 elements for articular cartilage, and 155 elements for ligaments.

In this study, LS_DYNA (Livermore Software Technology Corporation, Livermore, CA, USA) was employed for finite element analysis. Bone tissue was commonly considered an isotropic elastic material. The MAT_001 model was adopted to simulate the mechanical behavior of bones, with the following material properties: density of 1.5×10^{-9} g/mm^3, a Poisson's ratio of 0.3, and an elasticity modulus of 15000 MPa [37].

The mechanical behavior of ligaments, articular cartilage, and articular capsules was modeled using the Neo-Hookean model (MAT_007) [4]. This model, introduced in 1948, offered a simplistic representation of hyperelastic materials, akin to Hooke's law [23]. The strain energy function of the model is expressed as follows:

$$\Psi = C_{10}(I_1 - 3) + \frac{1}{D_1}(J-1)^2, \tag{1}$$

$$C_{10} = \frac{G}{2}, \tag{2}$$

$$D_1 = \frac{2}{K}, \tag{3}$$

where G represents the shear modulus and K represents the volume modulus. Since the human elbow ligament and articular capsule can be approximately incompressible materials, $J = 1$. The parameters C10 for ligaments, articular cartilage, and normal articular capsules were set at 1.790, 1.440 and 1.440 MPa, respectively [37]. Based on experimental data from Gao et al. [14], reflecting the shear modulus increase at various contracture stages, the parameters C10 were determined as 1.515, 1.610, 1.820 and 2.115 MPa at 2, 4, 6, and 8 weeks post-injury, respectively. Correspondingly, the thicknesses of the articular capsule

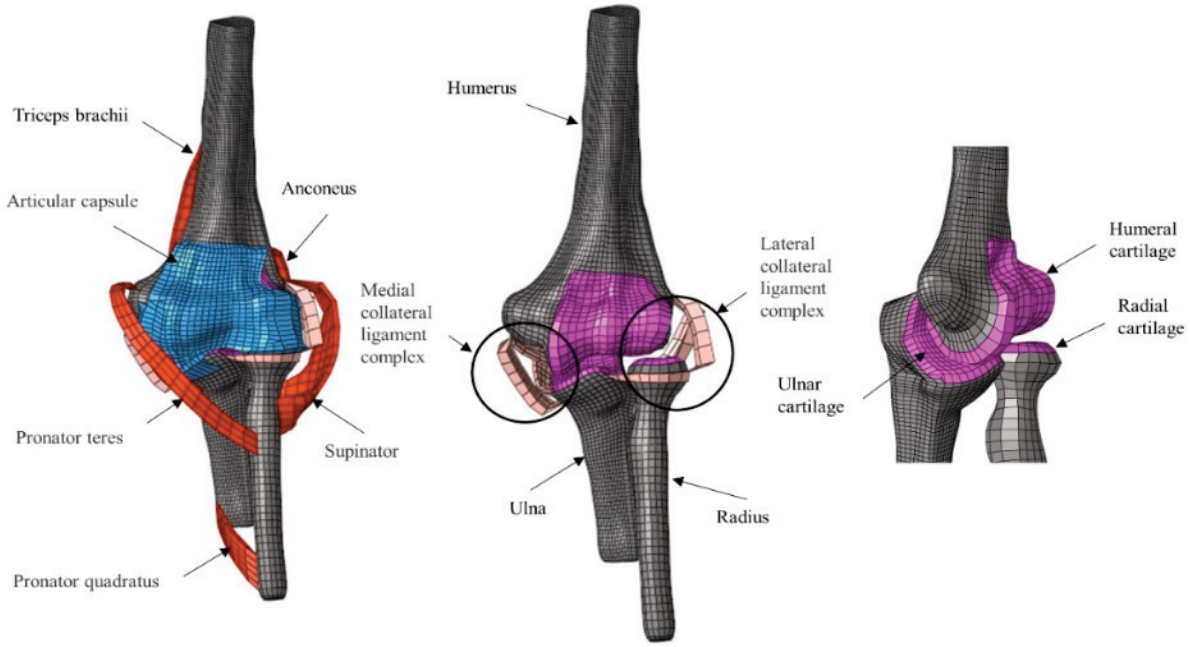

Fig. 1. Three-dimensional finite element model of the elbow joint

at these stages were 1.6, 2.5, 3.9 and 4 mm [10], [39].

Hedenstierna et al. [15] integrated QLV material and Hill truss material to develop a muscle model exhibiting both hyperelasticity and viscoelasticity. In our study, we utilized the combined passive QLV model (MAT_176) and active Hill model (MAT_156) for the skeletal muscle model. The active force equation is defined as follows:

$$F_{ce} = A(t)F_{\max}F_v(t)F_l(t)\,, \tag{4}$$

where $F_{\max}$ represents the muscle specific maximal isometric force, F_v represents a function of the relative contraction velocity, F_l represents a function of relative muscle length, and A represents the state of activation.

The instantaneous elastic response, the relaxation function of the viscous stress and the viscoelastic stress of the QLV model are given by:

$$\sigma_\varepsilon = \sum_i^k C_i \varepsilon^i\,, \tag{5}$$

$$G(t) = \sum_{i=1}^n G_i e^{-\beta_i t}\,, \tag{6}$$

$$\sigma = \int_0^t G(t-\tau)\frac{\partial \sigma^e}{\partial \varepsilon}\frac{\partial \varepsilon}{\partial \tau}\,, \tag{7}$$

where G_i represents the instantaneous shear modulus, β_i represents the decay constant. C_i represents the elastic constants. The value of i in G_i and β_i are four, and the value of i in C_i is three. The parameters of the Hill and QLV models are shown in Table 1.

Table 1. Parameters of Hill and QLV models

Parameter	Value
C_i	0.991; 0; 34.65
G_i/MPa	0.697; 1.086; 0.102; 0.1
β_i/s^{-1}	589.1; 312.4; 1; 4.5 × 10^{-3}

2.2. Verification of the elbow joint finite element model

The finite element model's static simulation was executed based on the boundary and loading conditions from the experiment conducted by Takatori et al. [31]. Von Mises stress measurements on the humeroradial joint contact surface of the elbow finite model were taken and compared to the results from Takatori et al. research. The model's validity was corroborated in an earlier study [37].

2.3. Flexion simulation in different stages of articular capsule after injury

During flexion, all ligaments and muscles were set to interact with their corresponding bones in a face-to-

face contact mode. The nodes at the distal humerus were restricted by six degrees of freedom. The angular velocity or rotation around the flexion axis was applied to the radius and ulna. The remaining five degrees of freedom of the ulna and radius were fixed, permitting the elbow joint to flex. Kodek et al. [22] investigated the dynamics of the elbow joint, measuring the velocity trajectory at various flexion angular speeds ranging from 0.25 rad/s to 1 rad/s. In our study, an angular velocity of 1 rad/s was selected to simulate flexion at different stages of anterior capsular contracture.

Table 2. Stiffness severity and passive range of motion at different stages

Stage	Stiffness	Passive range of motion [°]
Normal	no stiffness	0~90
2 weeks	minimally stiffness	0~90
4 weeks	moderately stiffness	0~75
6 weeks	severely stiffness	0~60
8 weeks	severely stiffness	0~60

Capsular contracture increased the stiffness of the articular capsule and restricted passive range of motion (ROM) of the joint [30]. In our research, drawing on Zhou's experiment [39], Beck's [3] and Carlock's findings [7], and Mansat's classification [24], passive range of motion and stiffness severity in the model was categorized at various stages of anterior capsular contracture, as depicted in Table 2.

3. Results

3.1. Stress changes to the ulnar cartilage post-injury

The trend of the stress curve for ulna cartilage was comparable under normal conditions, and at 2 weeks. In these scenarios, the stress of the ulna cartilage escalated with increasing flexion angle from 0 to 75° (Fig. 2A) and decreased from 75 to 90°. Under normal conditions, and at 2, and 4 weeks, the ulnar cartilage attained its peak stress at 75°. In normal conditions, the highest stress in the ulnar cartilage was 1.08 MPa, amounting to 1.02 times and 1.05 times the stress observed at 2 and 4 weeks, respectively. At 6 and 8 weeks, ulnar cartilage stress from 45 to 75° was lower compared to that measured in other conditions, with the peak stress being 0.70 and 0.68 MPa, respectively, indicating minimal variation.

3.2. Stress changes to the different ligaments post-injury

The MCL is comprised of anterior, posterior, and transverse bands. In every scenario, stress within the MCL, LUCL, and RCL intensified with elbow flexion (Fig. 2B–F). Throughout the joint contracture process, stress in the anterior bundle of the MCL (aMCL) and the transverse bundle of the MCL (tMCL) underwent significant changes, while stress in the posterior bundle of the MCL (pMCL) remained relatively stable. Under normal conditions, the peak stress of the aMCL was 3.95 MPa at 90°, closely matching the cadaveric experiment data of Debski et al. (4.3 MPa) [11]. At 15° flexion, the stress in the aMCL at 6 and 8 weeks began to fall below that in other conditions (Fig. 2B). Between 45 and 90°, the stress in the aMCL at 4 weeks was higher than that at 2 weeks. At 4 weeks, compared with 6 weeks, the stress of the anterior bundle at 15, 30, 45 and 60° was reduced by 11.1, 22.6, 37.3 and 36.1%, respectively. In the formation of capsular contracture, the aMCL stress always concentrated on the side adjacent to the articular capsule (Fig. 3), aligning with findings by Floris et al. [13], and the aMCL stress distribution were no visible changes in the tissue at different flexion angles. In all cases, the stress in the pMCL was consistently higher than in other ligaments (Fig. 4A–E), reaching its peak at the maximum flexion angle (Fig. 2C). The stress in the tMCL at 4 weeks was lower than in other conditions when the flexion angle exceeded 20° (Fig. 2D). For flexion angles greater than 30°, the stress in the tMCL at 6 and 8 weeks surpassed that at 4 weeks but remained below the levels observed in normal and 2 weeks conditions.

The lateral ligament complex of the elbow joint consists of the LUCL, RCL and AL [6]. When the flexion angle was less than approximately 47°, the stress in the LUCL changed minimally across all conditions (Fig. 2E). However, at flexion angles exceeding 47°, the stress in the LUCL at 2 weeks was lower than in other conditions. In all scenarios, the stress in the RCL increased with an increasing flexion angle (Fig. 2F), and at 4 weeks, its stress from 45° to 75° was higher than in other cases. The peak stress in the AL was reached at 75° flexion under normal conditions (Fig. 2G), at 2 weeks. In other cases, the stress in the AL peaked at the maximum flexion angle.

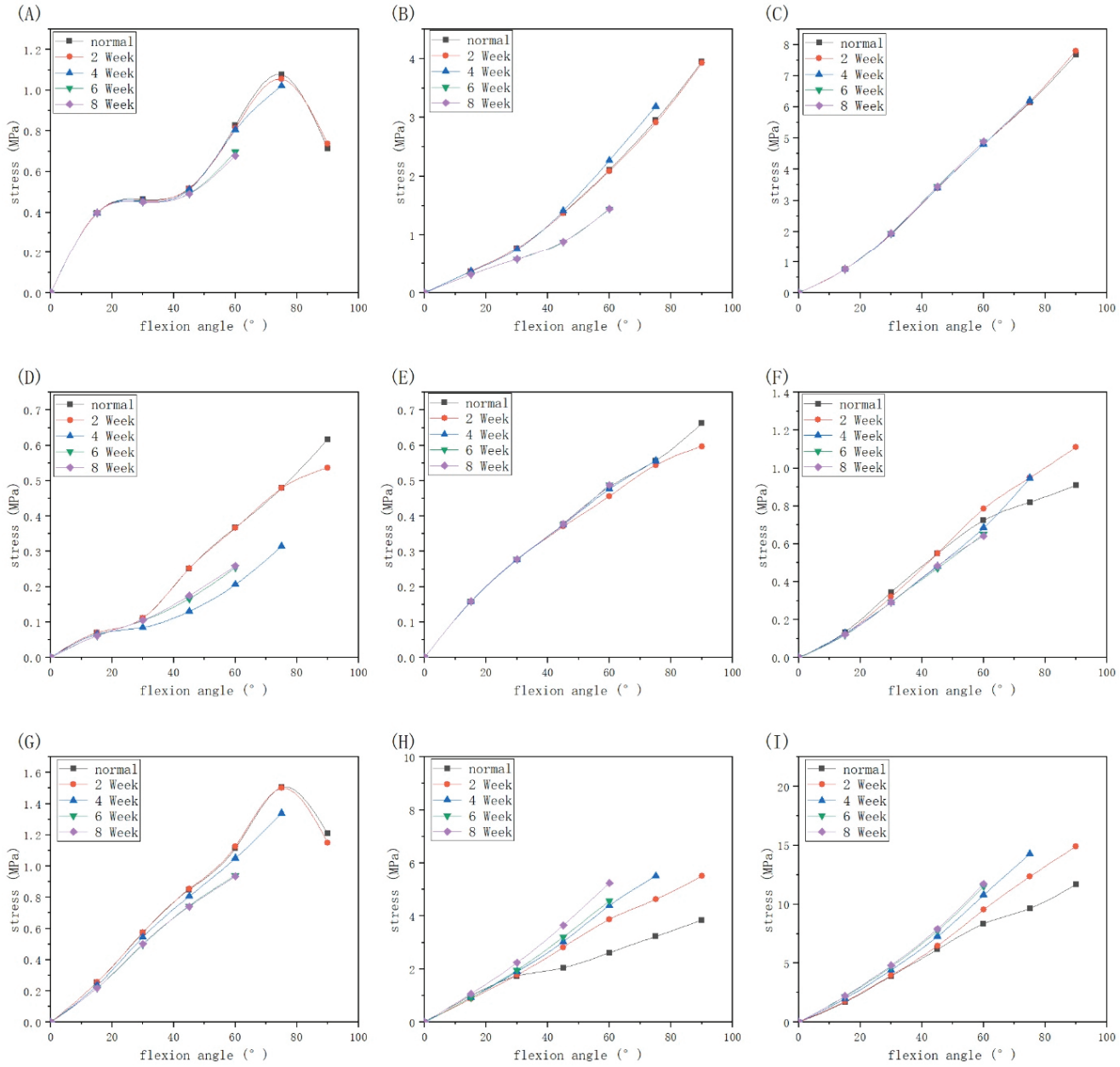

Fig. 2. Stress of the different soft tissue under all cases: (A) ulnar cartilage, (B) AMCL, (C) PMCL, (D) TMCL, (E)LUCL, (F) RCL, (G) AL, (H) anterior joint capsule, (I) posterior joint capsule

3.3. Stress changes to the articular capsule post-injury

During elbow flexion, stress in both the anterior and posterior joint capsules escalated over time (Fig. 2H and 2I), with peak stress occurring at the maximum flexion angle in all instances. While the flexion angle was 60°, stress of the anterior capsule was 2.62 MPa. Compared to no injury condition, stress on the anterior capsule increased by 47.7, 67.9, 74.3 and 100.0% at 2, 4, 6 and 8 weeks, respectively. At 6 and 8 weeks, the peak stress of the posterior articular capsule was 11.5 and 11.7 MPa (Fig. 2I), respectively, showing only a slight variation.

4. Discussion

In this study, reverse engineering was employed to create a finite element model that incorporates muscle activation behavior, simulating elbow flexion under normal conditions and various stages after anterior articular capsule injury. We analyzed the von Mises stress distribution and changes in different tissues during elbow

flexion to assess the biomechanical environment of the articular capsule and its surrounding tissues under diverse conditions.

Under normal conditions and at 2, 4, 6 and 8 weeks, the stress of pMCL was the highest during elbow flexion, followed by the stress of aMCL (Fig. 4A–E), indicating that the MCL was crucial for maintaining the motion stability of the elbow joint. The aMCL prevented cubitus valgus deformity [5], while the pMCL served as a secondary stabilizer during elbow flexion

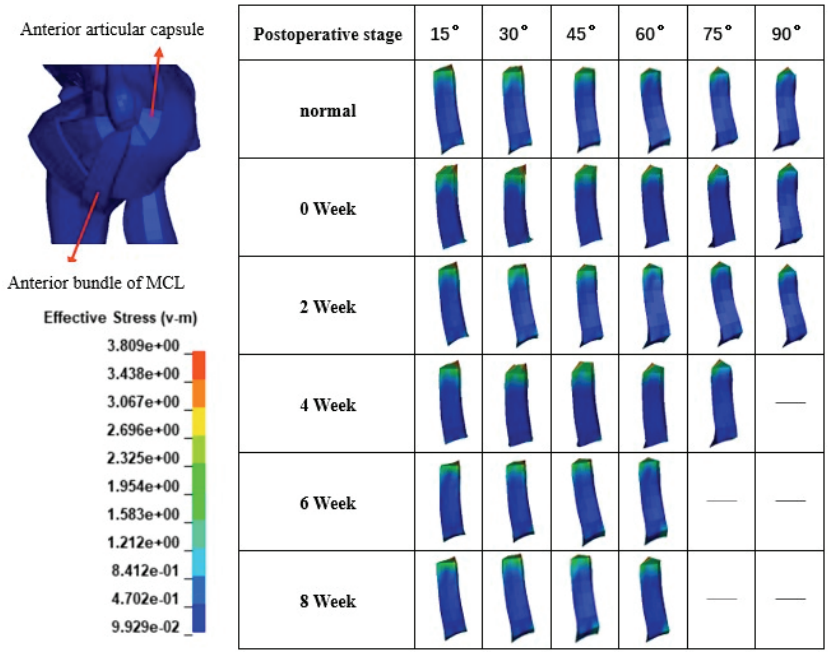

Fig. 3. Stress distribution on the aMCL under all cases

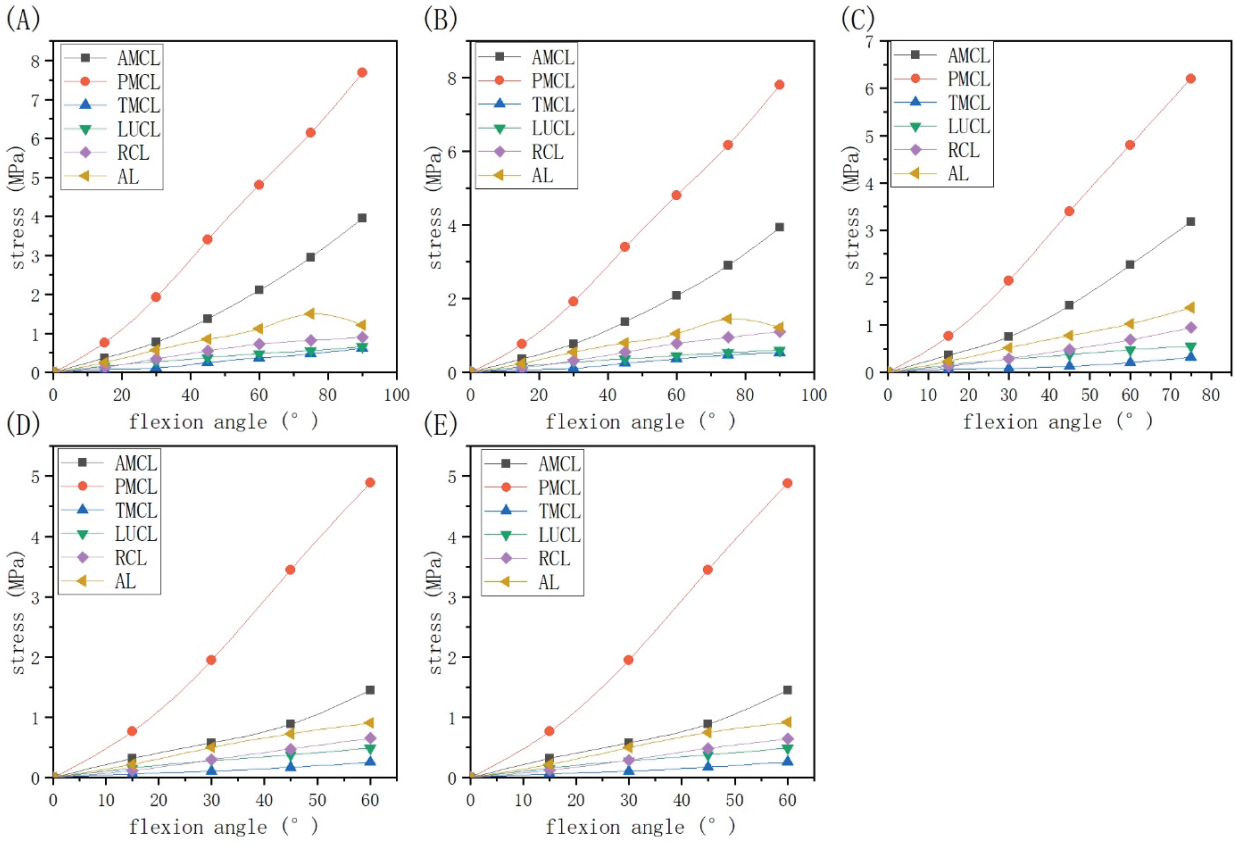

Fig. 4. Stress of all ligaments under different cases: (A) normal, (B) 2 weeks, (C) 4 weeks, (D) 6 weeks, (E) 8 weeks

[29], with the tMCL playing a lesser role [5]. Under normal conditions, the peak stress of the aMCL was 3.95 MPa at 90°, closely matching the cadaveric experiment data of Debski et al. (4.3 MPa) [11]. The stress in the aMCL predominantly concentrated on the side adjacent to the articular capsule (Fig. 3), aligning with findings by Floris et al. [13]. At 4 weeks, compared with 6 weeks, the stress of the anterior bundle at 15, 30, 45 and 60° was reduced by 11.1, 22.6, 37.3 and 36.1%, respectively. In the process of capsular contracture, the aMCL stress distribution were no visible changes (Fig. 3) and the aMCL stress gradually decreased from 4 weeks to 6 weeks (Fig. 2B). The stress of the aMCL was partially transferred to the articular capsule, thereby increasing the stress of the anterior articular capsule. As the elbow joint continued to contract, some of the aMCL's stress transferred to the anterior articular capsule, while the stress in the pMCL underwent slight changes. In all scenarios, the stress in the pMCL was significantly higher than in the other ligaments (Fig. 4A–E), underscoring its importance in maintaining elbow flexion during contracture. This finding was consistent with clinical observations by Jupiter et al. [19], who noted significant contracture of the pMCL in patients with limited elbow flexion.

We compared the stress values of ulnar cartilage under normal condition and at different stages of contracture. It was observed that at 4 weeks following anterior capsular injury, the peak stress of ulnar cartilage reduced by 5.6%, compared to the normal state. At 2 weeks, the peak stress of the articular cartilage was nearly equivalent to normal, at about 98.1%. This suggested that, prior to 2 weeks, the injured articular capsule was likely in the healing stages, aligning with findings by Cikes et al. [9]. They observed three patients with traumatic elbow stiffness and noted that local wound healing commenced within 2 weeks post-surgery.

Myofibroblasts were well-recognized for their crucial role in wound healing [25]. Following articular capsule injury, myofibroblasts utilized cellular contractile properties to minimize wound size during healing, and typically disappeared once wound recovery was complete. However, if the healing response became maladaptive, tissue fibrosis might occur [26]. Hildebrand et al. [16] in their study on a post-traumatic contracture animal model, noted early changes in the articular capsule by comparing the contracted knee with the control knee. They discovered a significant increase in the proportion of myofibroblasts to total cells at 4 weeks post-injury. Mirroring these findings in animal experiments, our study also yielded similar results mechanically. While the flexion angle was 60°, stress of the anterior capsule was 2.62 MPa. Compared to no injury condition, stress on the anterior capsule increased by 47.7, 67.9, 74.3 and 100.0% at 2, 4, 6 and 8 weeks, respectively. After 4 weeks, stress in the anterior joint capsule was on an upward trend when the flexion angle ranged from 30 to 90°. Mechanical signaling was vital for myofibroblast functionality, and increased intracellular stress was indicative of myofibroblast differentiation [34]. The heightened stress in the anterior articular capsule correlated with an increased presence of myofibroblasts within the capsule.

Generally, α-SMA is known to enhance tissue tension and facilitate wound contraction and healing during posttraumatic tissue healing [40]. In models of posttraumatic elbow contracture, α-SMA expression started to increase at 4 weeks post-injury, reaches its peak at 6 weeks, and then maintains a high level [16]. Elevated α-SMA expression indicated increased adhesion of fibrous tissue and is a key molecular factor in post-traumatic capsular contracture [40]. At 8 weeks, compared with 6 weeks, the peak stress of ulnar cartilage, tMCL, LUCL, RCL, AL and posterior capsule decreased by 2.8% (Fig. 2A), increased by 2.0% (Fig. 2D), decreased by 0.2% (Fig. 2E), decreased by 1.5% (Fig. 2F), decreased by 1.1% (Fig. 2G) and increased by 1.7% (Fig. 2I), respectively. At 6 weeks after anterior capsular injury, the stress in the ulnar cartilage, tMCL, LUCL, RCL, and AL posterior capsule showed little change at 0 to 60° flexion. This might relate to fibrosis in the anterior joint capsule at 6 weeks post-injury, leading to severe contracture. These observations align with clinical case results reviewed by Carlock et al. [7]. They reviewed 42 cases of elbow contracture, 29 of which exhibited severe elbow stiffness and a motion range not exceeding 60° at 6 weeks post-surgery.

Charalambos et al. [8] hypothesized that soft tissue contracture is a primary factor in joint contracture. The finite element simulation in this study was exclusively focused on anterior capsular contracture, excluding other soft tissue contractures such as those involving ligaments and muscles. Future research should consider improving the model, such as adding muscle and skin, and to further investigate the biomechanical response of other soft tissue contractures.

In addition, the finite element model of this study was based on CT data from healthy subject. The major limitation of this study is that the findings cannot be directly applied to patients with elbow contracture. In subsequent studies, clinical trials for verification are needed.

5. Conclusions

In this paper, we established an elbow joint model to assess the biomechanical environment of the elbow capsule and its surrounding tissues at various stages after anterior articular capsule injury. During anterior capsular contracture, the stress in the posterior bundle of the MCL was significantly higher than in other ligaments, underscoring its crucial role in elbow flexion. The stress in the anterior articular capsule increased at flexion angles of 30 to 90° after 2 weeks. At 6 and 8 weeks post-injury, the stresses in the ulnar cartilage, tMCL, LUCL, RCL, AL and posterior capsule exhibited minimal changes. These findings can aid rehabilitation doctors in understanding the biomechanical environment within the joint capsule and its surrounding tissues during joint contracture.

Acknowledgements

The authors thank the scholarship supported by National Natural Science Foundation of China (NSFC) Research Grants (12102301; 31871212; 51975411).

References

[1] ADOLFSSON L., *Post-traumatic stiff elbow*, EFORT Open Rev, 2018, 3 (5), 210–216, DOI: 10.1302/2058-5241.3.170062.

[2] BADIA A., STENNETT C., *Sports-related injuries of the elbow*, J. Hand Ther., 2006, 19 (2), 206–226, DOI: 10.1197/j.jht. 2006.02.006.

[3] BECK C.M., GLUCK M.J., ZHANG Y., MCGOUGH J.D., REIZNER W., RUBIN T.A., HAUSMAN M.R., *Outcomes of Arthroscopic Elbow Contracture Release: Improvement for Severe Prosupination and Flexion Contracture*, Arthroscopy, 2022, 38 (2), 315–322, DOI: 10.1016/j.arthro.2021.07.020.

[4] BUCHLER P., RAMANIRAKA N.A., RAKOTOMANANA L.R., IANNOTTI J.P., FARRON A., *A finite element model of the shoulder application to the comparison of normal and osteoarthritic joints*, Clin. Biomech., 2002, (9–10), 630–639, DOI: 10.1016/ S0268-0033(02)00106-7.

[5] CALLAWAY G.H., FIELD L.D., DENG X.H., TORZILLI P.A., WARREN R.F., *Biomechanical evaluation of the medial collateral ligament of the elbow*, J. Bone and Joint Surg. Am., 1997, 79 (8), 1223–1231.

[6] CAMP C.L., FU M., JAHANDAR H., DESAI V.S., SINATRO A.M., ALTCHEK D.W., DINES J.S., *The lateral collateral ligament complex of the elbow quantitative anatomic analysis of the lateral ulnar collateral, radial collateral, and annular ligaments*, J. Shoulder Elbow Surg., 2019, 28 (4), 665–670, DOI: 10.1016/j.jse.2018.09.019.

[7] CARLOCK K.D., BIANCO I.R., KUGELMAN D.N., KONDA S.R., EGOL K.A., *Risk Factors for Elbow Joint Contracture After Surgical Repair of Traumatic Elbow Fracture*, J. Am. Acad. Orthop. Surg., 2021, 29 (4), e178–187, DOI: 10.5435/jaaos-d-18-00801.

[8] CHARALAMBOUS C.P., MORREY B.F., *Posttraumatic elbow stiffness*, J. Bone Joint Surg. Am., 2012, 9, 1428–1437, DOI: 10.2106/JBJS.K.00711.

[9] CIKES A., JOLLES B.M., FARRON A., *Open Elbow Arthrolysis for Posttraumatic Elbow Stiffness*, J. Orthop. Traumatol., 2006, 20 (6), 405–409, DOI: 10.1097/00005131-200607000-00007.

[10] COHEN M.S., SCHIMMEL D., HASTINGS H. 2nd., MUEHLEMAN C., *Structural and biochemical evaluation of the elbow capsule after trauma*, J. Shoulder Elb. Surg., 2007, 16 (4), 484–490, DOI: 10.1016/j.jse.2006.06.018.

[11] DEBSKI R.E., WEISS J.A., NEWMAN W.J., MOORE S.M., MCMAHON P.J., *Stress and strain in the anterior band of the inferior glenohumeral ligament during a simulated clinical examination*, J. Shoulder Elb. Surg., 2005, 14 (1 Suppl. S), 24S–31S, DOI: 10.1016/j.jse.2004.10.003.

[12] DUNHAM C.L., CASTILE R.M., CHAMBERLAIN A.M., LAKE S.P., *The role of periar-ticular soft tissues in persistent motion loss in a rat model of posttrau-matic elbow contracture*, J. Bone Joint Surg. Am., 2019, 101, e17(1–7), DOI: 10.2106/ JBJS.18.00246.

[13] FLORIS S., OLSEN B.S., DALSTRA M., SLZRJBIERG J.O., SNEPPEN O., *The medial collateral ligament of the elbow joint: Anatomy and kinematics*, J. Shoulder Elbow Surg., 1998, 7 (4), 345–351, DOI: 10.1016/S1058-2746(98)90021-0.

[14] GAO Y., GAO B., ZHU H., YU Q., XIE F., CHEN C., LI Q., *Adipose-derived stem cells embedded in platelet-rich plasma scaffolds improve the texture of skin grafts in a rat full-thickness wound model*, Burns, 2020, 46 (2), 377–385, DOI: 10.1016/j.burns.2019.07. 041.

[15] HEDENSTIERNA S., HALLDIN P., BROLIN K., *Evaluation of a combination of continuum and truss finite elements in a model of passive and active muscle tissue*, Comput. Method Biomec., 2006, 11 (6), 627–639, DOI: 10.1080/17474230802312516.

[16] HILDEBRAND K.A., ZHANG M., GERMSCHEID N.M., WANG C, HART D.A., *Cellular, matrix, and growth factor components of the articular capsule are modified early in the process of posttraumatic contracture formation in a rabbit model*, Acta Orthop., 2008, 79 (1), 116–125, DOI: 10.1080/ 17453670710014860.

[17] HILDEBRAND K.A., ZHANG M., VAN SNELLENBERG W., KING G.J., HART D.A., *Myofibroblast numbers are elevated in human elbow capsules after trauma*, Clin. Orthop., 2004, 419, 189–197, DOI: 10.1097/00003086-200402000-00031.

[18] HINZ B., PHAN S.H., THANNICKAL V.J., GALLI A., BOCHATON--PIALLAT M., GABBIANI G., *The Myofibroblast: One Function, Multiple Origins*, Am. J. Pathol., 2007, 170 (6), 1807–1816, DOI: 10.2353/ajpath.2007.070112.

[19] JUPITER J.B., O'DRISCOLL S.W., COHEN M.S., *The assessment and management of the stiff elbow*, Instr. Course Lect., 2003, 52, 93–111.

[20] KAHMANN S.L., SAS A., GROßE HOKAMP N., VAN LENTHE G.H., MÜLLER L.P., WEGMANN K., *A combined experimental and finite element analysis of the human elbow under loads of daily living*, J. Biomech., 2023, 158, 111766, DOI: 10.1016/ j.jbiomech.2023.111766.

[21] KODDE L.F., VAN RIJN J., VAN DEN BEKEROM M.P., EYGENDAAL D., *Surgical treatment of post-traumatic elbow stiffness: a systematic review*, J. Shoulder Elb. Surg., 2013, 22 (4), 574–580, DOI: 10.1016/j.jse.2012.11.010.

[22] KODEK T., MUNIH M., *An analysis of static and dynamic joint torques in elbow flexion-extension movements*, Simul. Model Pract. Th., 2003, 11 (3–4), 297–311, DOI: 10.1016/ S1569-190X(03)00063-7.

[23] KUMARA V., MISHRAA R.K., KRISHNAPILLAI S., *Study of pilot's comfortness in the cockpit seat of a flight simulator*, Int. J. Ind. Ergonom., 2019, 71, 1–7, DOI: 10.1016/j.ergon. 2019.02.004.

[24] MANSAT P., MORREY B.F., *The column procedure: a limited lateral approach for extrinsic contracture of the elbow*, J. Bone Joint Surg. Am., 1998, 80 (11), 1603–1615.

[25] MONIKA P., WAIKER P.V., CHANDRAPRABHA M.N., RANGARAJAN A., CHIDAMBARA K.N., *Myofibroblast Progeny in Wound Biology and Wound Healing Studies*, Wound Repair Regen., 2021, 29 (4), 531–547, DOI: 10.1111/wrr.12937.

[26] MONUMENT M.J., HART D.A., SALO P.T., HILDEBRAND K.A., BEFUS A.D., *Posttraumatic elbow contractures: targeting neuroinflammatory fibrogenic mechanisms*, J. Orthop. Sci., 2013, 18 (6), 869–877, DOI: 10.1007/s00776-013-0447-5.

[27] O'DRISCOLL S.W., BELL D.F., MORREY B.F., *Posterolateral rotatory instability of the elbow*, J. Bone Joint Surg. Am., 1991, 73 (3), 440–446.

[28] RODRIGUEZ-MARTIN J., PRETELL-MAZZINI J., ANDRES--ESTEBAN E.M., LARRAINZAR-GARIJO R., *Outcomes after terrible triads of the elbow treated with the current surgical protocols. A review*, International Orthopaedics, 2013, 851–860, DOI: 10.1007/s00264-010-1024-6.

[29] SHUKLA D.R., GOLAN E., WEISER M.C., NASSER P., CHOUEKA J., HAUSMAN M., *The posterior bundle's effect on posteromedial elbow instability after a transverse coronoid fracture: A biomechanical study*, J. Hand Surg. Am., 2018, 43 (4), 381–388, DOI: 10.1016/j.jhsa. 2017.09.018.

[30] SUNG E.J., CHUN M.H., HONG J.Y., DO K.H., *Effects of a resting foot splint in early brain injury patients*, Ann. Rehabil. Med., 2016, 40 (1), 135–141, DOI: 10.5535/arm.2016.40.1. 135.

[31] TAKATORI K., HASHIZUME H., WAKE H., INOUE H., NAGAYAMA N., *Analysis of stress distribution in the humeroradial joint*, J. Orthop. Sci., 2002, 7 (6), 650–657, DOI: 10.1007/ s007760200116.

[32] TAN J., WU J., *Current progress in understanding the molecular pathogenesis of burn scar contracture*, Burns Trauma, 2017, 5, 14, DOI: 10.1186/s41038-017-0080-1.

[33] TRUDEL G., UHTHOFF H.K., BROWN M., *Extent and direction of joint motion limitation after prolonged immobility: An experimental study in the rat*, Arch. Phys. Med., 1999, 80 (12), 1542–1547, DOI: 10.1016/S0003-9993(99)90328-3.

[34] VAN DE WATER L., VARNEY S., TOMASEK J.J., *Mechanoregulation of the Myofibroblast in Wound Contraction, Scarring, and Fibrosis: Opportunities for New Therapeutic Intervention*, Adv. Wound Care, 2013, 2 (4), 122–141, DOI: 10.1089/wound.2012.0393.

[35] VELTMAN E.S., DOORNBERG J.N., EYGENDAAL D., VAN DEN BEKEROM M.P., *Static progressive versus dynamic splinting for posttraumatic elbow stiffness: a systematic review of 232 patients*, Arch. Orthop. Trauma Surg., 2015, 135, 613–617, DOI: 10.1007/s00402-015-2199-5.

[36] WAHL E.P., LAMPLEY A.J., CHEN A,. ADAMS S.B., NETTLES D.L., RICHARD M.J., *Inflammatory cytokines and matrix metalloproteinases in the synovial fluid after intra-articular elbow fracture*, J. Shoulder Elb. Surg., 2020, 29 (4), 736–742, DOI: 10.1016/j.jse. 2019.09.024.

[37] WANG F., WANG H., LI M., JIA S., WANG J., ZHANG J., FAN Y., *The role of the joint capsule in the stability of the elbow joint*, Med. Biol. Eng. Comput., 2023, 61, 1439–1448, DOI: 10.1007/ s11517-023-02774-6.

[38] ZHANG D., NAZARIAN A., RODRIGUEZ E.K., *Post-traumatic elbow stiffness: Pathogenesis and current treatments*, Shoulder Elbow, 2020, 12 (1), 38–45, DOI: 10.1177/ 1758573218793903.

[39] ZHOU Y., ZHANG Q.B., ZHONG H.Z., LIU Y., LI J., LV H., JING J.H., *Rabbit Model of Extending Knee Joint Contracture: Progression of Joint Motion Restriction and Subsequent Joint Capsule Changes after Immobilization*, J. Knee Surg., 2020, 33 (01), 015–021, DOI: 10.1055/s-0038-1676502.

[40] ZHUANG Z., YU D., CHEN Z., LIU D., YUAN G., YIRONG N., SUN L., LIU Y., HE R., WANG K., *Curcumin Inhibits Joint Contracture through PTEN Demethylation and Targeting PI3K/Akt/mTOR Pathway in Myofibroblasts from Human Joint Capsule*, Evid-Based Compl. Alt, 2019, 2019, 1–12, DOI: 10.1155/2019/4301238.